Arabian Journal of Geosciences (2020) 13: 357
https://doi.org/10.1007/s12517-020-05378-8

ORIGINAL PAPER

Site response assessment and ground conditions at King Saud University Campus, Riyadh City, Saudi Arabia

Sattam A. Almadani[1] · Kamal Abdelrahman[1,2] · Fahad I. bin Mansour[3]

Received: 23 September 2018 / Accepted: 28 April 2020 / Published online: 14 May 2020

Abstract
Site response characteristics have a significant influence on ground motion vibrations. To evaluate the site response effects at King Saud University campus, the horizontal-to-vertical spectral ratio (HVSR) technique has been applied at 45 sites with about 400-m spacing. The recording time was more than 1 h at each site with a sampling rate of 100 Hz. The data were processed and analyzed using Geopsy software to produce measurements of fundamental frequency and minimum site amplification factor. Moreover, shear-wave velocity down to 30-m depth has been acquired at 10 measuring sites in the campus. In addition, geotechnical borehole data were collected from four boreholes within the campus. Generally, in majority of sites the H/V curve for amplitude spectra displayed a clear peak, signifying the presence of a sharp soil–bedrock impedance contrast between alluvial deposits and underlying bedrock. It is indicated that the fundamental frequency ranges between 0.64 and 1.94 Hz. Given the measured resonance frequency of around 1 Hz, buildings located on the alluvium that have 5 stories in height could experience soil-structure resonance, while the amplification factor varies from 1.19 to 11.22 indicating localized zones having high vulnerability index due to the considerable thickness of alluvial deposits. Moreover, shear-wave velocity ranges between 320 m/s and 684 m/s revealing zones of stiff soil to very dense soil/or soft rock which is correlated well with the geotechnical parameters of borehole data. Based on these results, the ground conditions of near-surface sediments in the King Saud University campus indicate weak zones that led to ground subsidence resulting in differential settlements of foundations.

Keywords Site response · Resonance frequency · Amplification · Vulnerability · Riyadh · Saudi Arabia

Introduction

Various types of surface layers can influence ground motion due to differences in soil hardness and thickness. In general, soft soil sites tend to have lower shear-wave velocities and to amplify ground motions relative to hard rock sites. The damage level may also be associated with a combination of building height and shallow subsurface velocity structure. When earthquakes occur, columns of ground materials may vibrate stronger in a certain frequency range. Buildings may also vibrate at a higher amplitude in a certain frequency range. When both frequencies are similar, soil structure resonance will occur and the potential damage to the building will be increased. For a more efficient approach, we use records of ground motion of noise to measure site response parameters. Microtremors are ground vibrations (Susilo and Wiyono 2012) resulted from either natural or artificial sources and reflect the shallow geological conditions. Ventura et al. (2004) estimated the site period with experimental and analytical studies of microtremors in British Columbia. Noor and Daud (2016) determined soil thickness based on the natural frequency of microtremor ambient vibrations conducted at the Universiti Tun Hussein Onn Malaysia (UTHM). Microtremors were measured at five boreholes at UTHM to verify the correlation between the natural frequency (f_0) and borehole depth. Fnais et al. (2010) collected microtremor data at 85 sites distributed regularly through the Yanbu metropolitan area in western Saudi Arabia to evaluate the site response effect of soil within the city's urban area. Abdelrahman et al.(2012) conducted

Responsible Editor: Abdullah Al-Amri

✉ Sattam A. Almadani
salmadani@ksu.edu.sa

1 Geology and Geophysics Department, King Saud University, Riyadh, Saudi Arabia

2 Seismology Dep., National Research Institute of Astronomy and Geophysics, Cairo, Egypt

3 King Abdullah City for Atomic and Renewable Energy (KACARE), Riyadh, Saudi Arabia

seismic microzonation for New Domiat City, northern Egypt using microtremor measurements.

King Saud University is the oldest university in the Kingdom of Saudi Arabia where it was established in 1957 in Riyadh City (Fig. 1). The university has many medical, scientific, and humanitarian research programs that accommodate thousands of students each year. Because the university is continuously developing, the university is keen to expand the modern scientific disciplines and incorporate them in the university educational system, which requires constructing new buildings, facilities, and infrastructures. The university was built on weathered bedrock, and the topsoil of sand and gravel overlays layers of weathered limestone that suffers from geotechnical problems. In addition, the limestone hosts abundant caves and joints filled with marl and soft materials. We therefore carried out numerous experiments to determine site response parameters at many locations across campus and created maps to show the lateral variation of these parameters. The ground vulnerability index has been calculated as well in the King Saud University campus. Moreover, the borehole geotechnical data for four drilled boreholes in the campus have been collected and analyzed (Table 1).

Geological setting

The Riyadh quadrangle is covered by Phanerozoic sedimentary rocks (El-Asa‘ad 1984; Vaslet et al. 1991). The Phanerozoic succession is unconformably overlain by Late Tertiary to Quaternary deposits (Fig. 2). Most of the campus structures are founded on Arab Formation Members C, D and Jubaila Limestone covered by alluvium and gravel deposits. Based on the borehole data, the near-surface sediments of KSU campus consist of three layers from top to bottom: (1) silty sand with gravel; (2) completely weathered limestone; and (3) weathered limestone interbedded with thin layers of silty sand (below the top layer of BH-3 borehole).

The Jubaila Limestone are the oldest rocks being of early Kimmeridgian age (from 157 MA to 152 MA) and are composed of 118.3 m (in the type section) of partially dolomitized aphanitic limestones in the lower 85 m and calcarenitic limestones in the upper 33 m (Powers 1968). The Jubaila Formation is described as medium strong to strong (depending on the weathering grade) dark gray and pale gray, mud-rich and grain-rich carbonate rocks. Arab Formation was divided by Manivit et al. (1985) into informal units Ja + Jha, Jad + Jac and Jad (Fig. 3). The Arab

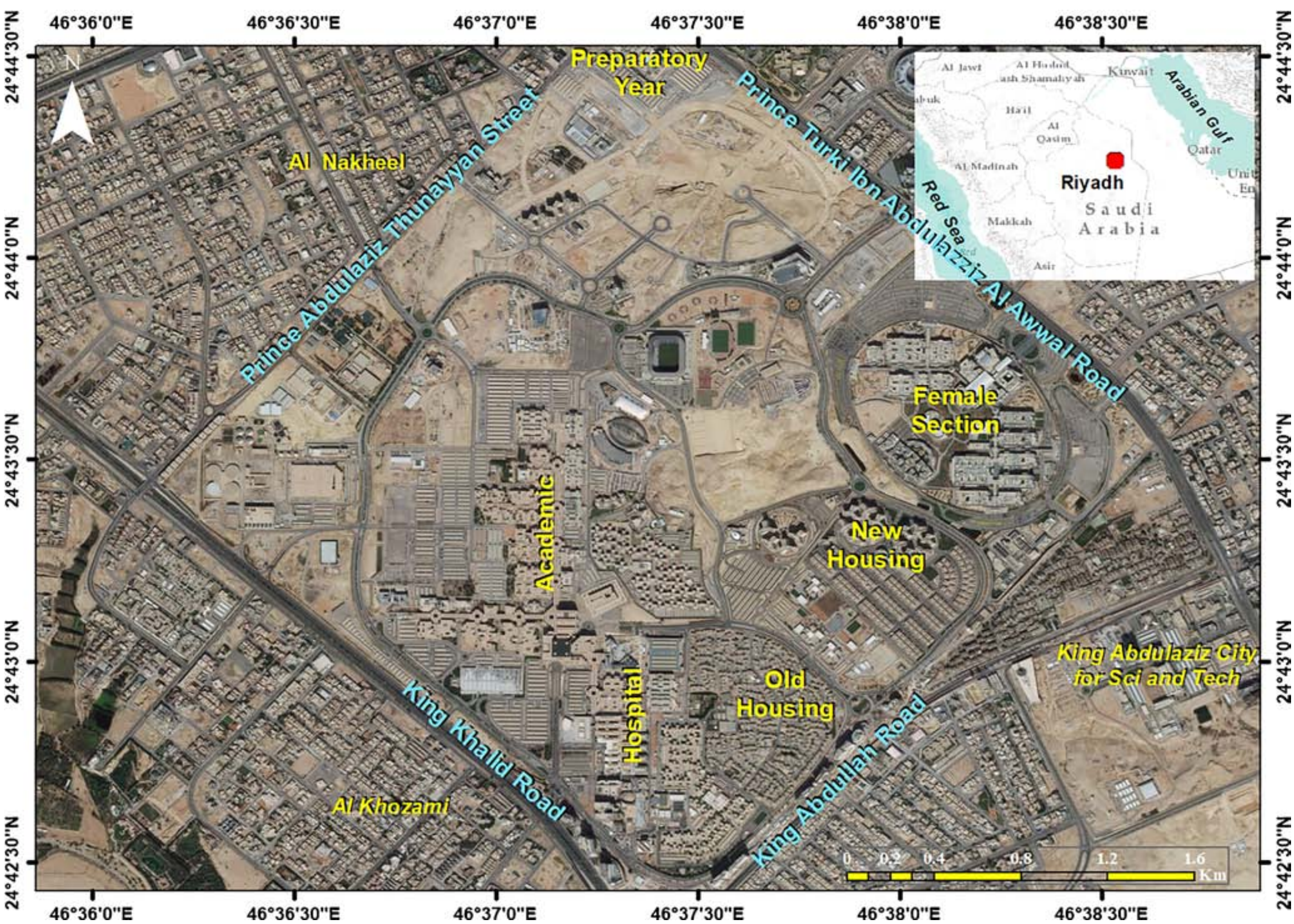

Fig. 1 Location map of King Saud University campus

Table 1 Geotechnical parameters of borehole No. 1

Depth (m)	Description	SPT (N)	W.C. (%)	L.L. (%)	P.I. (%)	REC. (%)	RQD (%)
0	Silty sand with gravel (brown, very dense, dry)	100	17	-	NP		
0.5	Limestone interbedded with thin layers of silty						
1.0	sand (creamy, highly weathered, very highly					53	12
1.5	fractured						
2.0						49	16
2.5							
3.0							
3.5							
4.0						55	19
4.5							
5.0							
5.5						63	21
6.0	End of borehole						

Formation rests conformably on the Jubaila Formation and is of Tithonian and Kimmeridgian age (from 152 MA to 145 MA) and comprises four shallowing-upward cycles of carbonate to evaporate; Arab D to Arab A form bottom to top. During the Miocene (about 13 MA) there was a change in climate and an onset of tectonic uplift which caused a change in the hydrological regime a subsequent dissolution of the anhydrite layer and collapse of the overlying limestone bed above (Vincent 2008).

Since deposition, the limestone formations have been affected by diagenesis and tectonism. This is evident in the dissolution of the anhydrite layers in the Arab Formation and the development of secondary porosity and secondary permeability within the rock mass. These characteristics include microfractures, fossil molds, solution vugs, and secondary permeability by formation of fractures which widen into connected channels. The rock is heterogeneous on all scales and the change in rock mass characteristics across a section can be very rapid. The Sulaiy Formation is composed of thinly bedded nodular chalky lime mudstone with interbedded peloidal–ooidal and skeletal packstone/grainstone. The Quaternary deposits (< 2.6 MA) found on site are likely to be interbedded by alluvium composed of red brown clay, silt and sand that varies from loose to dense (AECOM 2014) and Aeolian deposits fine sand and coarse silt.

Hydrogeologically, in arid regions, where the average annual rainfall is less than 200 mm, rainfall occurs as irregular high-intensity, short-duration precipitation events. Groundwater

Fig. 2 Regional stratigraphy of Riyadh City (Powers 1966)

Era	Period	Epoch	Formation	Lithology	Typical Thickness (m)
Cenozoic		Recent	Made Ground	Variable	Variable
	Pleistocene	Holocene-Pleistocene	Alluvium	Sandy silt and silty sand with gravel bands deposited within channels. Sand lenses present.	Variable
			Aeolian Deposits	Well rounded sands and silts deposited by wind.	
Mesozoic	Early Cretaceous	Berriasian-Valanginian	Sulaiy Formation	Aphanitic limestone. Intensely disturbed due to dissolution of the underlying Hith Anhydrite.	170m
	Late Jurassic	Tithonian	Lower Part of the Arab Formation: Upper Breccia Complex Arab C member Lower Breccia Complex Arab D member	Calcarenite and Aphanitic Limestone, Dolomite and some Anhydrite. Solution-collapse Carbonate Breccia due to loss of Anhydrite.	124m
		Kimmeridgian	Jubaila Formation	Aphanitic Limestone and Dolomite. Subordinate Calcarenite and Calcarenite Limestone.	118m

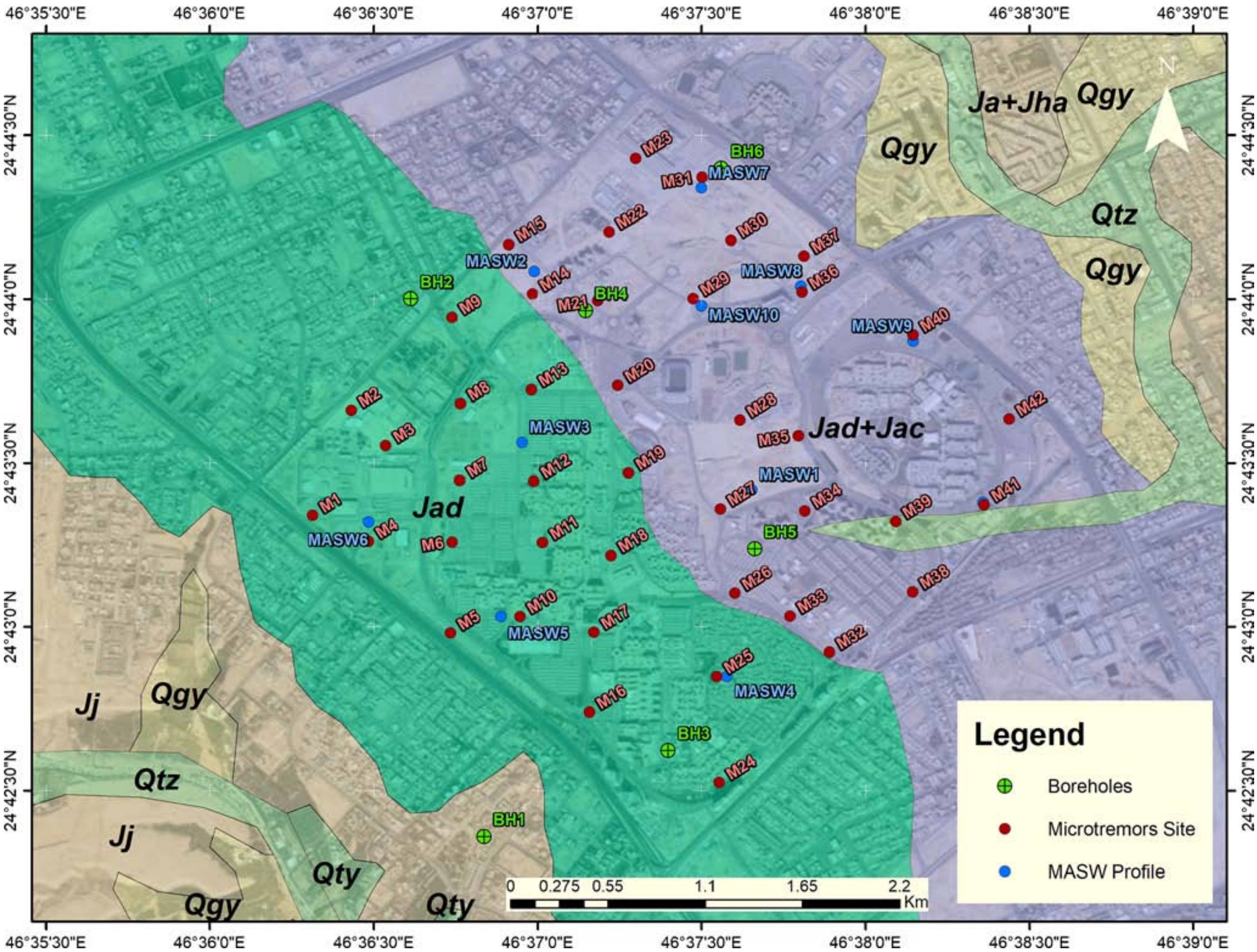

Fig. 3 Geologic map for the study area

recharge is generally limited to infiltration during the intermittent inundation of usually dry wadi channels. Dissolution associated with karst development has created a complex hydrogeology which is not associated with other sedimentary sequences. Groundwater levels may be subject to seasonal variation and fluctuations associated with irrigation, surface infiltration, and from leaking sewers and water mains into rock fractures resulting in perched and or rising perched water tables. The Jubaila Formation is identified as a regional city-wide aquifer and is classified as a secondary aquifer. Groundwater levels in the Jubaila Formation may be subject to seasonal variations, and may be sub-artesian and connected through vertical and horizontal discontinuities to the Arab Formation.

Data acquisition and processing

There are different types of data collected throughout this study including microtremor measurements, geotechnical borehole data, and multichannel analysis of surface waves (MASW) (Fig. 4). These integrated data were treated according to flowchart in Fig. 5.

Microtremor data

The horizontal-to-vertical spectral ratio (HVSR) approach has been applied using background noise (microtremors) to determine site response parameters such as fundamental frequency and site amplification. This well-established method is based on a computation of the ratio of horizontal ground motion over vertical motion.

Microtremor data was collected using a Taurus digital seismograph (Nanometrics Company) equipped with a three-component Trillium compact seismometer coupled with a field laptop computer. These data were acquired from February 2–25, 2017. The 45 measurement sites covered almost the entire study area (Fig. 4) at 400-m spacing. The recording period was continuous for 1 h at a 100-Hz sampling rate for each recording site (360,000 samples) after midnight to mitigate the influence of synthetic noise on the recorded signals. These data were acquired according to the

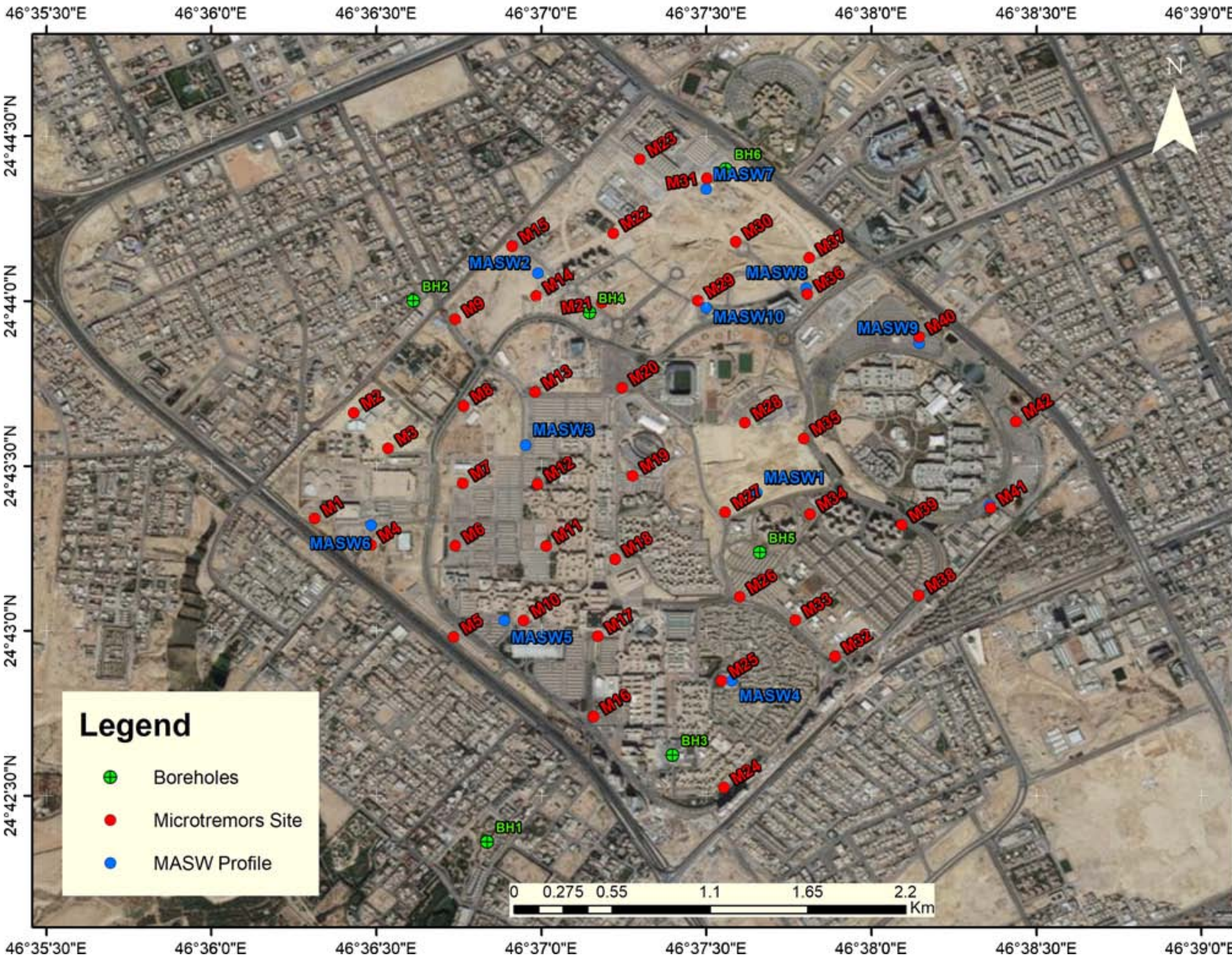

Fig. 4 Location of microtremors, boreholes, and MASW sites of measurements

Fig. 5 The methodology flowchart

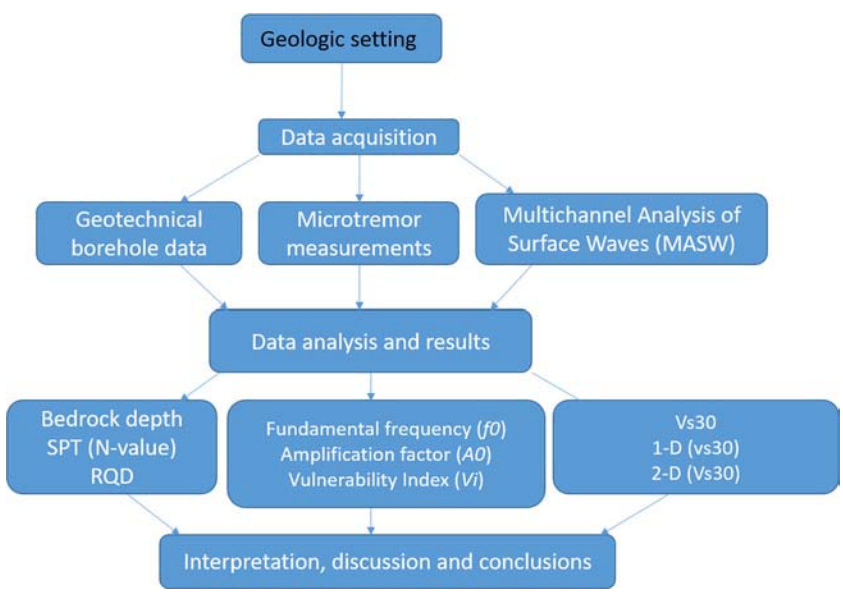

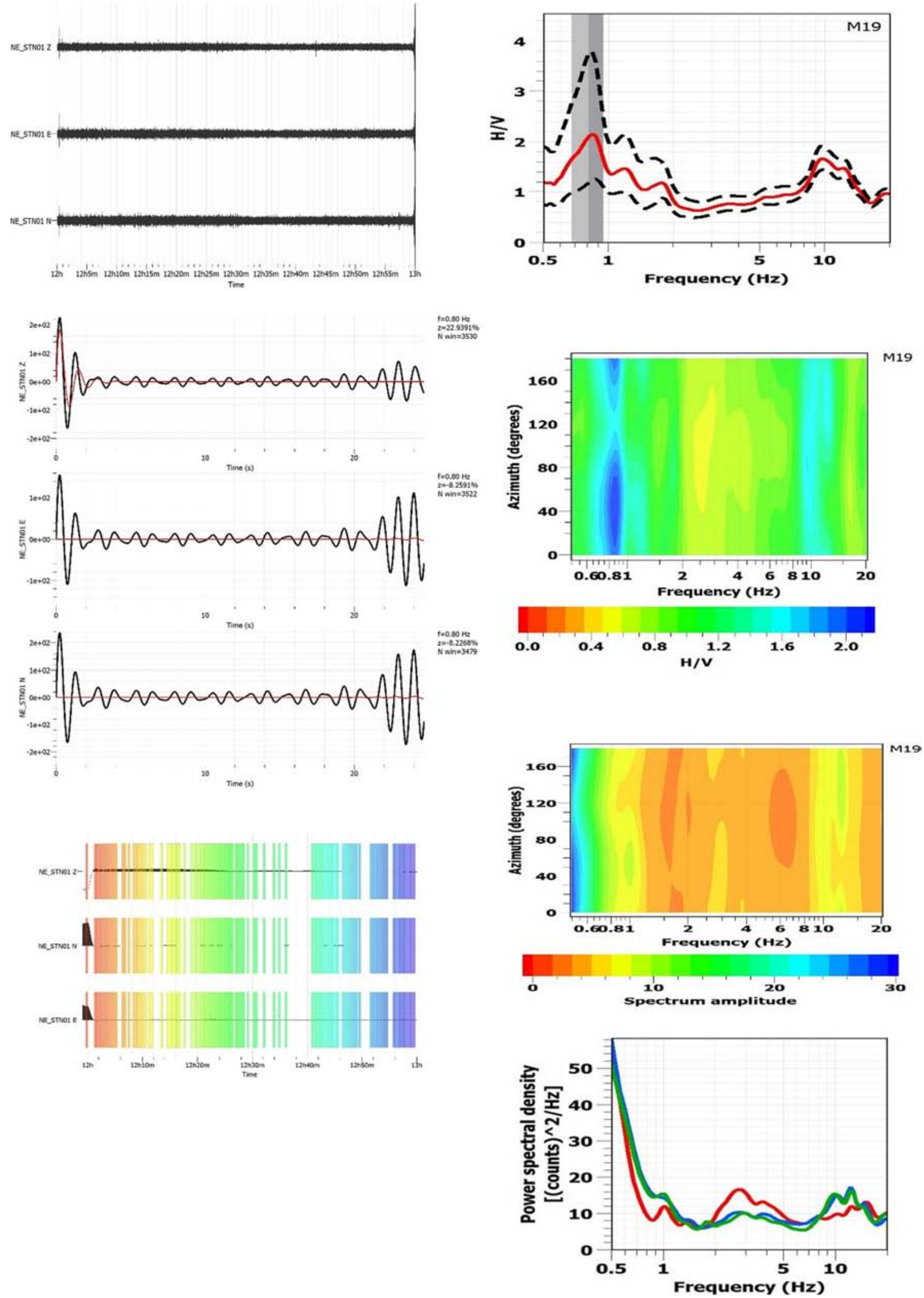

Fig. 6 Sequence processing steps of microtremor data for site M19

recommendations of the SESAME project (2004) and Bard (2007) based on the characteristics of the sensor and site. The seismometer coupled well with the bedrock with short external wiring avoiding mechanical and electronic interferences.

Table 2 Geotechnical parameters of borehole No. 2

Depth (m)	Description	SPT (N)	W.C. (%)	L.L. (%)	P.I. (%)	REC. (%)	RQD (%)
0	Silty sand with gravel (light brown, very dense, dry)	100	28	-	NP	55	26
0.5	Limestone interbedded with thin layers of silty sand (moderately weathered, highly to slightly fractured)						
1							
1.5						78	39
2.0							
2.5							
3.0							
3.5						100	67
4.0							
4.5							
5.0						100	85
5.5							
6.0	End of borehole						

The measurements during windy and rainy times have been avoided taking into account the considerable distance from the artificial noise sources.

The acquired data was processed using Geopsy software. The spectral ratios were calculated within frequency range from 0.2 to 20 Hz using a 25-s time window, and the artificial noise, e.g., from industrial and traffic sources, has been eliminated. The Konno and Ohmachi (1998) algorithm and cosine taper with 0.5% width were used for Fourier amplitude spectra smoothing using smoothing constant of 40 for the bandwidth. DC suppression was carried out to eliminate the instrumental effect. The Konno–Ohmachi algorithm is provided in the following equation:

$$W_B(f,\ f_c) = \frac{\sin\left(log_{10}\left(\frac{f}{fc}\right)^b\right)}{\left(log_{10}\left(\frac{f}{fc}\right)4\right)} \tag{1}$$

where:

f = frequency

fc = the central frequency for smoothing

b = bandwidth coefficient

To obtain the spectral ratio of the horizontal and vertical components, the two horizontal components must be one value, using the average of the square, before dividing by the

Table 3 Geotechnical parameters of borehole No. 3

Depth (m)	Description	SPT (N)	W.C. (%)	L.L. (%)	P.I. (%)	REC. (%)	RQD (%)
0	Silty sand with gravel (brown, medium dense, dry)			-	NP		
0.5		11	1.9				
1.0							
1.5		13	2.3				
2.0							
2.5	Limestone (creamy, highly weathered, very highly to highly fractured)					25	0
3.0							
3.5							
4.0						50	13
4.5							
5.0							
5.5							
6.0						60	40
6.5							
7.0							
7.5	End of borehole					70	47

Table 4 Geotechnical parameters of borehole No. 4

Depth (m)	Description	SPT (N)	W.C. (%)	L.L. (%)	P.I (%)	REC (%)	RQD (%)
0	Clean fill materials	100					
0.5							
1.0	Silty Gravel with sand	16					
1.5				21			
2.0	Silty clayey sand with gravel	12					
2.5							
3.0	Silty gravel with sand	20					
3.5							
4.0	Silty gravel with sand	24					
4.5							
5.0	Silty gravel with sand	27					
5.5							
6.0	Silty gravel with sand	30					
6.5							
7.0							
7.5		18					
8.0							
8.5		25					
9.0							
9.5		25					
10.0							
10.5		32					
11.0	Silty gravel with sand						
11.5		100					
12.0	Silty gravel with sand						
12.5							
13.0							
13.5	Limestone (creamy, moderately weathered,	100					
14.0	moderately fractured					90	70
14.5							
15.0	End of borehole						

vertical component. This process is performed for every selected window. The spectral ratio value of H/V is obtained from the average ratio of H/V for the selected windows (Fig. 6). H/V curves often exhibit local narrow peaks in urban areas. In most cases, such peaks usually have an industrial origin, related to some type of machinery, e.g., turbines or generators. Guidelines proposed by the SESAME European project (2004) and (Dunand et al. 2002) were applied to verify the clarity of H/V peaks on the KSU campus.

The soil vulnerability index, K_g, was also evaluated using the following equation:

$$K_g = A_0^2/f_0 \quad (2)$$

Table 5 Correlation between SPT-N value and Relative density (Meyerhof 1956)

SPT N-value(blows/0.3 m-1 ft)	Soil packing	Relative density (%)
< 4	Very loose	< 20
4–10	Loose	20–40
10–30	medium	40–60
30–50	Dense	60–80
> 50	Very dense	> 80

Table 6 RQD values for various joint densities along drill cores (Deere 1989)

Rock quality designation (RQD)	Description of rock quality
0–25 %	Very poor (completely weathered)
25–50%	Poor (weathered rock)
50–75 %	Fair (moderately weathered rock)
75–90%	Good (hard rock)
90–100 %	Excellent (fresh rock)

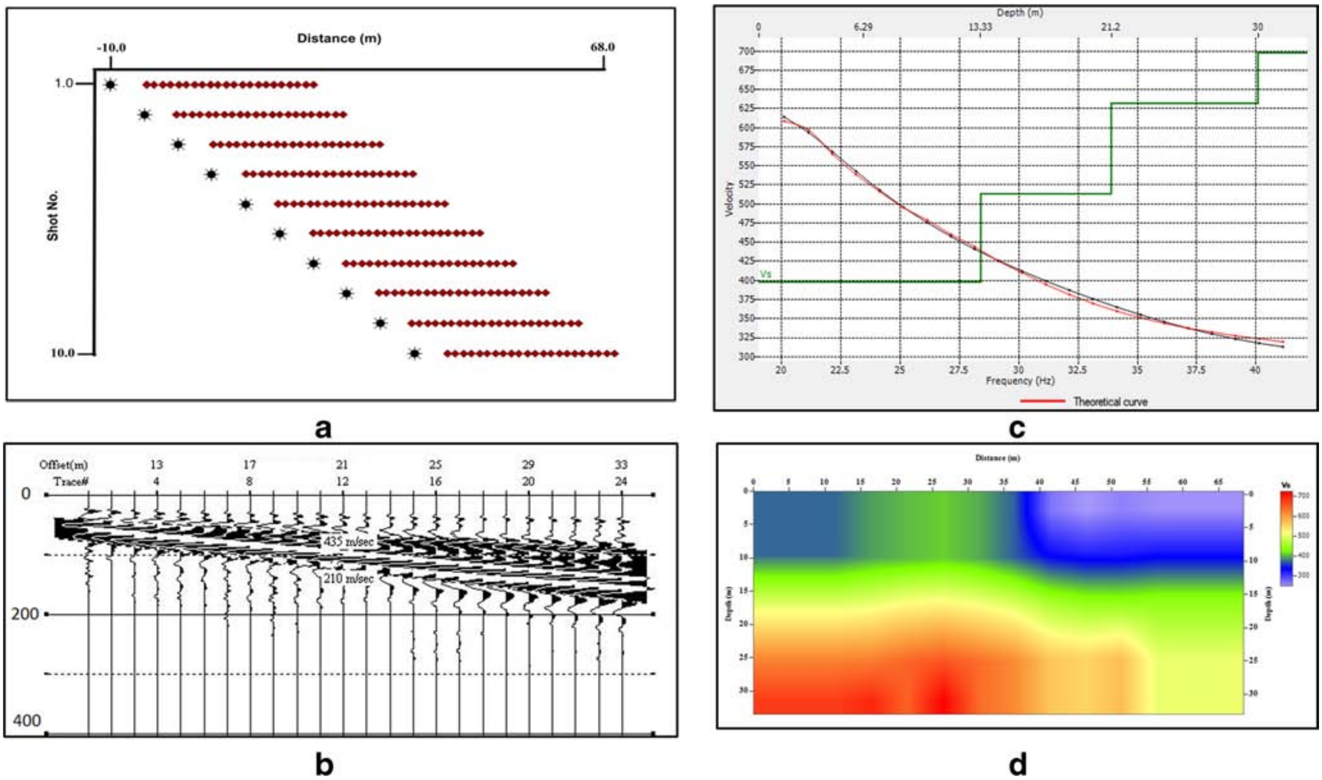

Fig. 7 Processing of MASW data in the present study

where A_0 is the site amplification. f_0 is fundamental frequency. The reclaimed land area suffered severe damage, and the k-value calculated for sites in this region had the highest value.

Borehole geotechnical data

The best way to understand subsurface geology is through applying invasive site assessment techniques such as drilling and trenching. Borehole geology has a great impact on the environment and involves other logistical issues that are associated with drilling in developed urban areas. Four boreholes were drilled inside the campus of King Saud University distributed throughout the campus, and another borehole was drilled close to the campus (Fig. 4; SAFCO 2014). The depth of these boreholes varies from 6 to 15 m below the ground surface according to the purposes of these boreholes. The groundwater level is recorded in two boreholes where the water depth is 4.3 m in borehole No. 2, while it is at 2 m in borehole No. 3. The geotechnical parameters of these boreholes are presented in Tables 2, 3, 4, and 5.

The standard penetration test (SPT) or "N-value" is an in situ dynamic penetration test designed to provide information on the geotechnical engineering properties of soil. The N-value provides an indication of the relative density of the subsurface soil and is used in empirical geotechnical correlations to estimate the approximate shear strength properties of the soils (Meyerhof 1956) according to Table 6. The rock quality designation (RQD) index has been used for over 20 years as an indicator of rock quality. It measures the percentage of good rock within a borehole. It is now used as a standard parameter in drill core logging and forms a basic element of several rock mass classification systems (Barton et al. 1974; Deere 1989). The rock quality designation (RQD) is a commonly used index for describing fractured rock masses or jointing degree, where RQD = 0 at joint intercepts (distance between the joints in the drill cores) of 10 cm or less, while RQD = 100 for distances of 11 cm or more. The RQD was initially introduced for civil engineering applications and has been quickly adopted in mining, engineering geology, and geotechnical engineering (Lucian and Wangwe 2013)

Multichannel analysis of surface waves

Multichannel analysis of surface waves (MASW) measurements were acquired by Geode seismograph (Geometrics Co.) equipped by 24 vertical geophones of 4.5 Hz using sledgehammer as energy source at 11 of selected sites (Fig. 4). The recorded waves were analyzed using *RadExPro* software to calculate shear-wave velocity down to 30 meters' depth (Vs30) through three processing steps as follows; (i) field-data preparation, (ii) dispersion-curve construction, and finally, (iii) inversion process. Field data were gathered with 1-m geophone spacing (Fig. 7). The energy source was

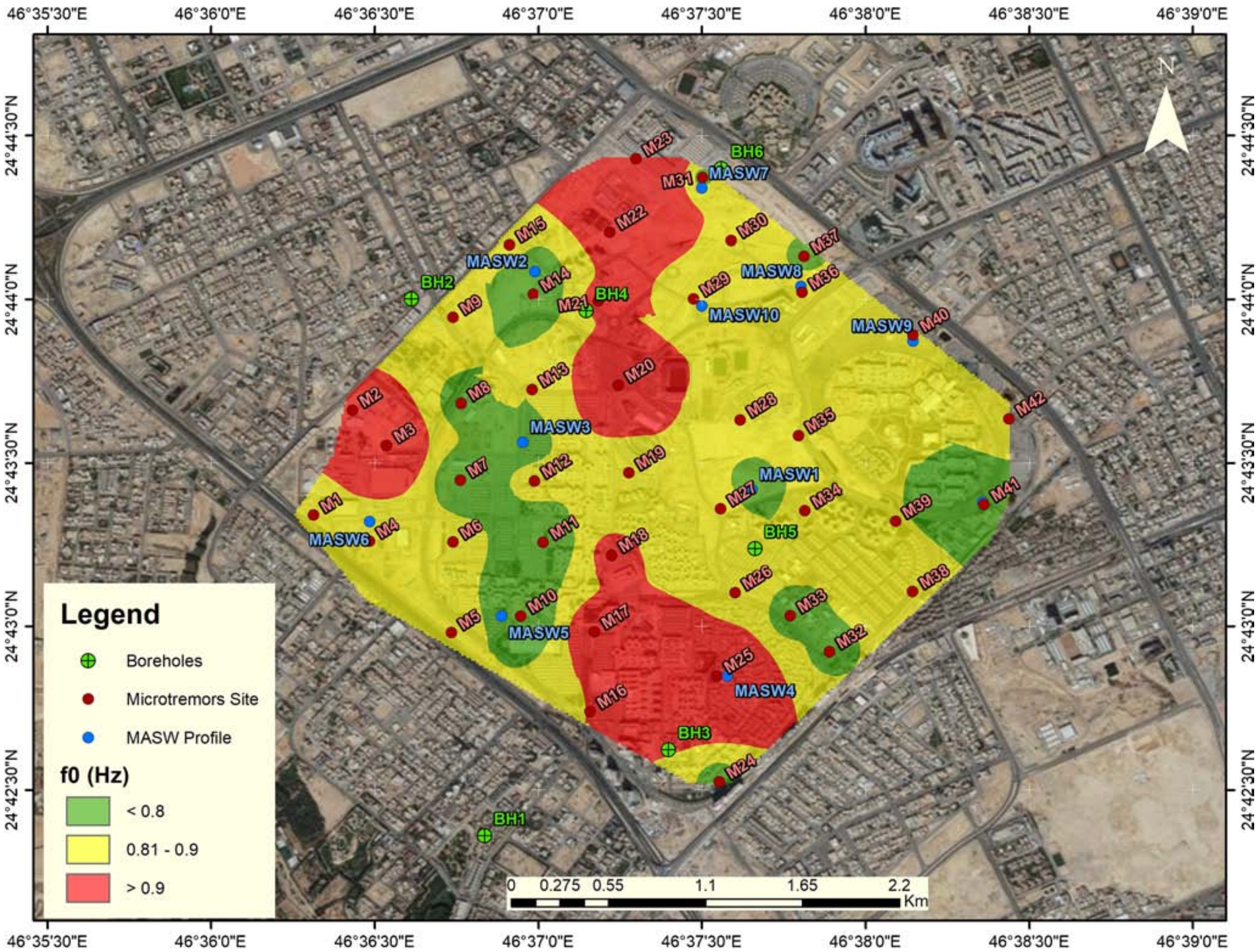

Fig. 8 Fundamental frequency f_0 distribution in King Saud University campus

sustained at a distance of 10 m for recording high-quality signals. Then, shear-wave velocity model was assessed through the inversion process based on least-squares fitting algorithm as follows.

The average shear-wave velocity for the depth "d" of soil is referred as V_H as follows; the average shear-wave velocity up to a depth of H (V_H) is computed as:

$$V_H = \sum d_i / \sum \left({}^{d_i}/_{v_i} \right) \tag{3}$$

where $H = \sum d_i$ = cumulative depth in meters.

For 30-m average depth, shear-wave velocity is written as:

$$V_{s(30)} = \frac{30}{\sum_{i=1}^{N} \left({}^{d_i}/_{v_i} \right)} \tag{4}$$

where d_i and v_i denote the thickness (in meters) and shear-wave velocity in m/s of the ith layer, respectively.

But for the borehole locations, the data is available for less than 30 m, (Vs30) was calculated using the "extrapolation assuming constant velocity" extrapolation method as proposed by Boore (2013) for boreholes of less than 30-m depth.

$$v_{s(30)=30/}\left(tt\left(d \right) + (30-d)/v_{\mathrm{eff}} \right) \tag{5}$$

where V_{eff} is the assumed effective velocity from depth d to 30 m and equals the velocity at the bottom of the velocity model:

$$v_{\mathrm{eff}} = v_{s(d)} \tag{6}$$

Results and interpretation

The collected broadband waveform data from 45 sites located across the King Saud University campus with sites spaced about 400 m apart as shown in Fig. 4 were analyzed through Geopsy software. After completing the data processing and analyses, the maximum H/V amplitudes and corresponding resonance frequencies were obtained for the 45 measurement

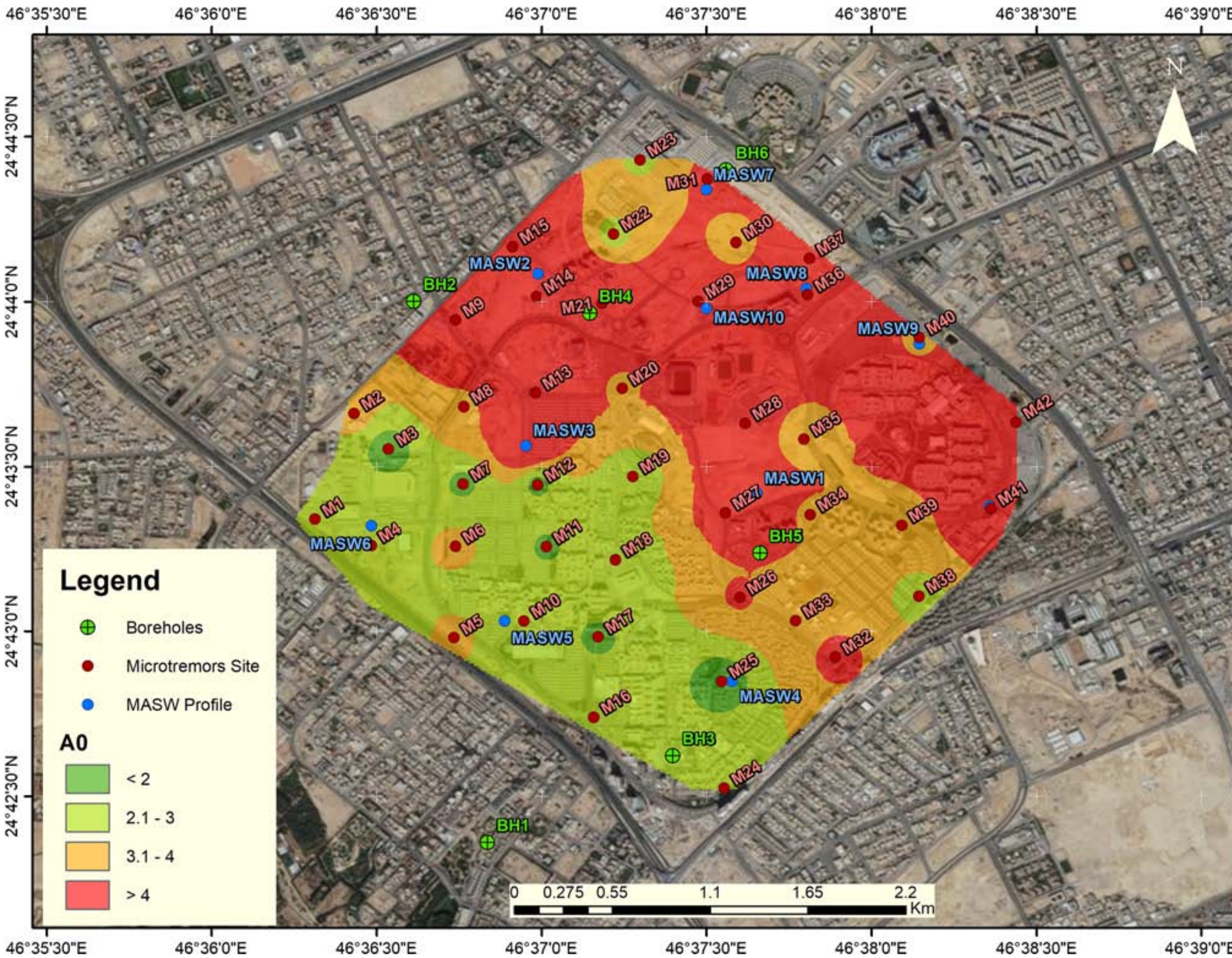

Fig. 9 Amplification factor A_0 distribution in King Saud University campus

locations. The f_0 values span from 0.64 and 1.95 Hz. In the current study, the majority of sites (90%) have f_0 less than 1 Hz, while the remaining 10% are more than 1 Hz. Then, we generated peak frequency map and peak amplitude map. The contour map of f_0 (Fig. 8) illustrates that high-frequency values appear in the north-eastern part of the campus, adjacent to the preparatory year buildings, indicating the presence of bedrock at shallow depths compared with other sites inside the campus. Another area with moderate f_0 values is found at the old faculty housing. Taking into account both the height of a building and its fundamental frequency of vibration, the effects of fundamental frequency (f_0) could be of great importance. In order to reduce the ground motion vibrations on these structures, the following equation (Shehata and Das 2019) can be used:

$$f_0 = 1\left(\mathrm{C_t}{*}\mathrm{H}^{3/4}\right) \tag{7}$$

where $\mathrm{C_t}$ is a factor determined according to the structural system and building material, and H is the height of the building (m), from the foundation or from the top of a rigid basement. Therefore, the structures inside the KSU campus should be designed to have a resonance frequency inconsistent with the fundamental frequency of the soil.

Based on a comparison of the general characteristics of the measured H/V curves that are considered reliable based on the criteria from SESAME. The A_0 values range from 1.19 to 11.22 (Fig. 9). In general, the 45 H/V curves are categorized into the following: (i) 9 H/V curves (20 %) with flat and broad peaks and amplitudes less than 2; (ii) 19 H/V curves (42.22%) with clear peaks and amplitudes from 2 to 5; (iii) 9 H/V curves (20 %) with peak amplitudes ranging from 5 to 10; and (iv) 9 H/V curves (17.77 %) with peak amplitudes greater than 10. These clear peaks indicate a sharp impedance contrast between alluvial sediments and the underlying limestone. The A_0 contour map indicates that the higher H/V peaks were obtained in the area between M31 and M37, near Prince Turki Ibn Abdulaziz Al Awwal road, while the area from M29 to M27 has moderate A_0 values.

The ground vulnerability index, kg-factor, map was also generated (Fig. 10) based on calculations of this factor at each

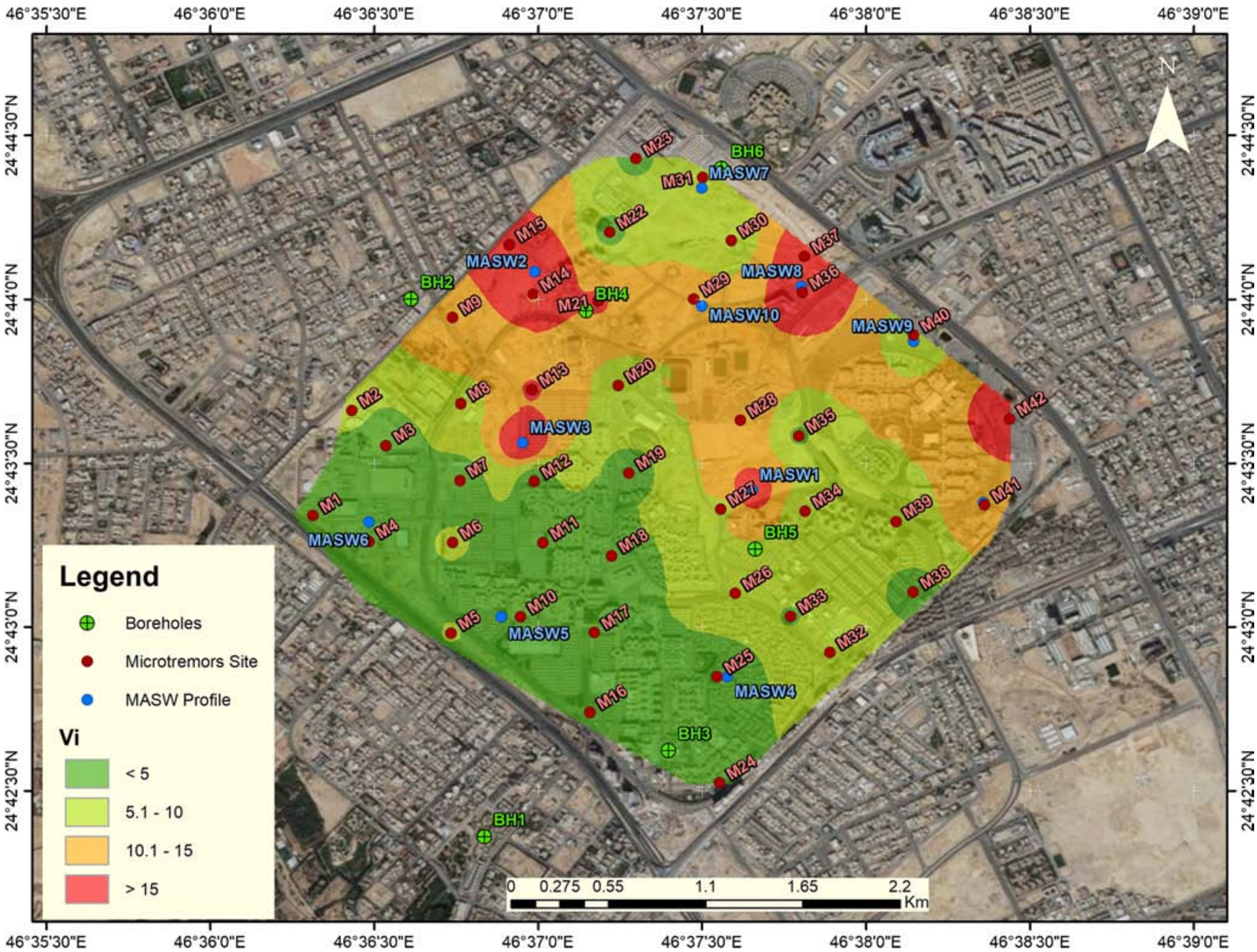

Fig. 10 Vulnerability index V_i distribution in King Saud University campus

site from the peak amplitude and frequency values. The seismic vulnerability index distribution in the area of study ranges from 0.84 to 25.27. Furthermore, there are some localized sites that have high susceptibility values (greater than 15) as M14, M15, M21, M27, M36, M37, and M42 extending along northeast–west direction through the campus.

Based on borehole data, the subsurface geologic setting at the site consists of three layers that extend from the ground surface to depths of 13.5 m; the topmost layer composed of silty sand with gravel (brown, medium dense, dry). This layer has thicknesses ranging from 0.5 to 2.0 m; limestone interbedded with thin layers of silty sand (creamy, highly weathered, and very highly fractured) below the top layer. The depth of this layer varies from 0.5 to 5.0 m; limestone (creamy, moderately weathered, moderately fractured) below the top layer in the BH-4 borehole. The depth of this layer was recorded as 13.5 m. Moreover, the shear-wave velocity down to 30-m depth (Vs30) at the locations of boreholes was calculated using Eq. 4, where the Vs(30) varies between 309 m/s and 595 m/s.

Figure 11 reveals the estimated shear-wave velocities at the MASW and borehole sites, where Vs(30) ranges from 320 m/s to 684.88 m/s. This figure illustrates that the northeastern, southwestern zones and a narrow zone extending northwest–southeast have Vs(30) greater than 360 m/s which is considered very dense soil or soft rock according to NEHRP recommendations, while the rest area of the campus has Vs(30) less than 360 m/s which means stiff soil or alluvium deposits.

Discussions and conclusions

Based on the results of microtremor measurements (f_0 and A_0), the narrow zone of high f_0 (greater than 0.9 Hz) that extends northwest–southeast across the campus indicates the shallow depth of limestone bedrock relative to the rest areas of the campus, whereas the A_0 map shows that the northern part of the campus has higher values of amplification factor indicating the presence of bedrock at greater depth than the southern part of the campus. This may also indicate the limestone itself

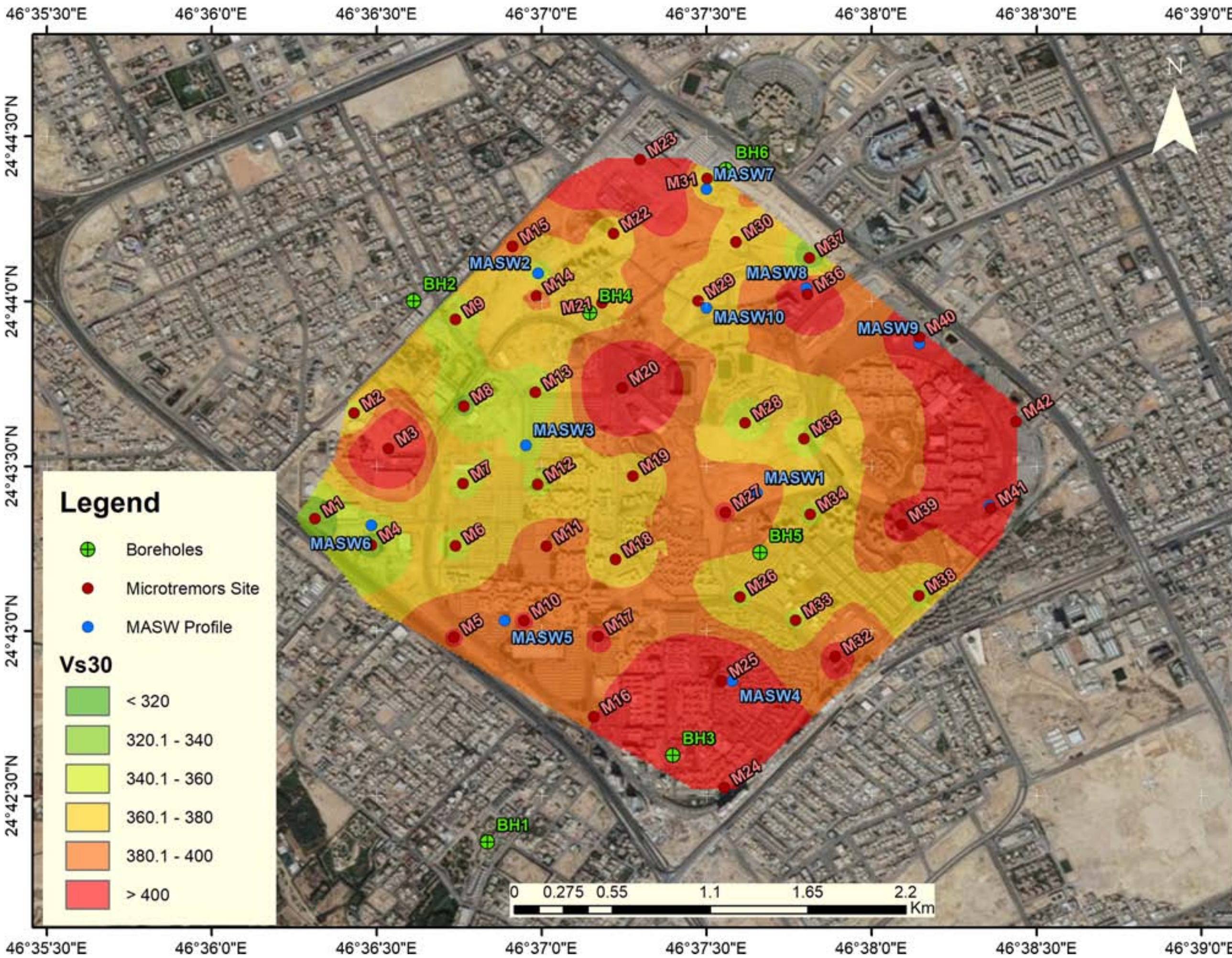

Fig. 11 Shear-wave velocity (Vs_{30}) distribution through KSU campus

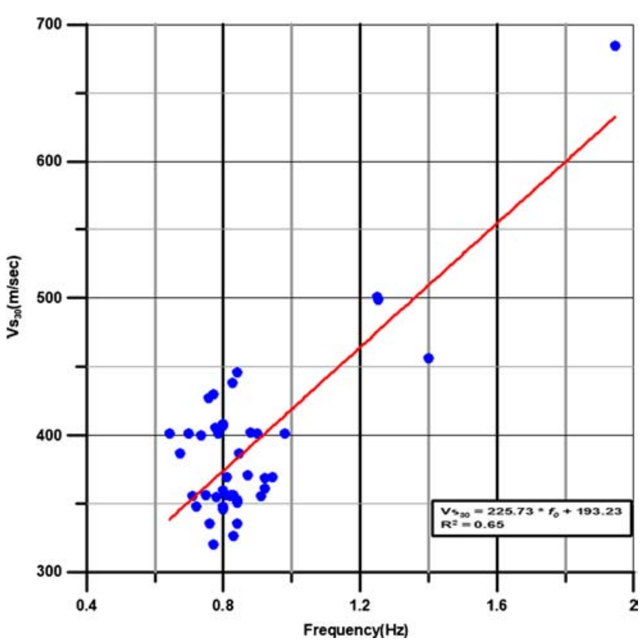

Fig. 12 The relationship between Vs_{30} and f_0 through the collected data

includes interbedded thin layers of silty sand as indicated by borehole geotechnical data.

Moreover, the relationship between *Vs(30)* and f_0 was studied (Fig. 12). This figure indicates the estimated relationship between both parameters as follows;

$$Vs_{30} = 225.73 * f_0 + 193.23 \tag{8}$$

There is a good correlation between these parameters where the correlation coefficient (R^2) of about 0.7 is acceptable statistically. This indicates the confidence level of the parameters of data acquisition and analyses. This map shows the near-surface sediments in the northern part of campus composed of stiff soil according to NEHRP recommendations (where it is covered by sediments with Vs less than 360 m/s) than the southern part constituted by very dense soil and soft rock (where it is covered by sediments with Vs in the range from 360 m/s to 684.88 m/s).

The available geotechnical borehole data in KSU campus identified the presence of alluvium sand and gravel sediments overlying either completely weathered, moderately weathered, or moderately fractured limestone bedrock layers. Based on data in Table 5, the quality of limestone in boreholes No. 1 and 3 is very poor, while the quality ranges from poor to fair at boreholes No. 2 and 4, which explains the higher H/V amplitudes at boreholes 1 and 3. Based on these results, the foundation layer of King Saud University campus has to be tested geotechnically before building where the quality of these rocks is very poor especially at BH-1 (for the whole penetrated depth), BH-2 (till 0.5-m depth), and BH-6 (till 6.0-m depth), which should be taken into account when planning future expansion.

Acknowledgments Deep thanks are extended to the reviewers for their beneficial review and valuable comments.

Funding information The authors would like to extend their sincere appreciation to the Deanship of Scientific Research at King Saud University for its funding this research group No. RGP -1436-010.

References

Abdelrahman K, Abd El-Aal A, El-Hady S, Mohamed A, Abdel-Moniem E (2012) Fundamental site frequency estimation at New Domiat city, Egypt. Arab J Geosci 5:653–661. https://doi.org/10.1007/s12517-010-0222-2

AECOM. Riyadh Metro Project Package 1: Geotechnical Interpretive Report. 2014.

Bard PY (2007) International training course on: seismology, seismic data analysis, hazard assessment and risk mitigation. Potsdam, Germany, pp 17–22

Barton NR, Lien R, Lunde J (1974) Engineering classification of rock masses for the design of tunnel support. Rock Mech 6(4):189–236

Boore DM (2013) The uses and limitations of the square-root-impedance method for computing site amplification. Bull Seismol Soc Am 103(4):2356–2368. https://doi.org/10.1785/0120120283

Deere DU (1989) Rock quality designation (RQD) after 20 years, U.S. Army Corps Engrs. Contract Report GL-89-1. Vicksburg, MS: Waterways Experimental Station.

Dunand F, Bard P Y, Chatelain J L, Guéguen P, Vassail T and Farsi M N (2002) Damping and frequency from random method applied to insitu measurements of ambient vibrations: evidence for effective soil structure interaction. 12th European Conference on Earthquake Engineering, London. p. 869.

El-Asa'ad G (1984) The paleobiogeographic distribution of the Late Cretaceous fauna of Arabia and surrounding areas. Arab Gulf J Sci Res 2(1):105–121

Fnais MS, Abdelrahman K, Al-Amri AM (2010) Microtremor measurements in Yanbu city of Western Saudi Arabia: A tool for seismic microzonation. Journal of King Saud University - Science 22(2):97–110

Konno K, Ohmachi T (1998) Ground-motion characteristics estimated from spectral ratio between horizontal and vertical components of microtremors: Bulletin of the Seismological Society of America 88, p. 228–241.

Lucian C, Wangwe EM (2013) The usefulness of rock quality designation (RQD) in determining strength of the rock. Int Refereed J Eng Sci 2(9):36–40

Manivit J, Pellaton C, Vaslet D, Le Nindre YM, Brosse JM, Breton JP, Fourniguet J (1985) Geologic map of the Darma' quadrangle, sheet 24 H, Kingdom of Saudi Arabia (with text): Saudi Arabian Deputy Ministry for Mineral Resources, Jeddah, Geoscience Map GM-101A.

Meyerhof G (1956) Penetration tests and bearing capacity of cohesionless soils. J Soils Mechanics and Foundation Division ASCE, 82(SM1).

Noor M, Daud M (2016) Determination of soil thickness based on natural frequency using microtremor measurement. ARPN Journal of Engineering and Applied Sciences. 11(8): 5342–5346

Powers RW (1966) Geology of the Arabian Peninsula. Sedimentary geology of Saudi Arabia. U.S, Geological Survey Professional Paper

Powers RW (1968) Lexique stratigraphique international: Saudi Arabia: vol. III, Asie, fasc. 10 b 1: Centre National de la Recherche Scientifique, Paris, 177 p.

SESAME Project (2004) Site effects using ambient excitations. URL: http://sesame-fp5.obs.ujf-grenoble.en. Accessed on May 1, 2017.

Shehata H, Das B (Eds.) (2019) GeoMEast 2018, SUCI, pp. 21–39. https://doi.org/10.1007/978-3-030-01923-5_3

Soil and Foundation Company (SAFCO) report (2014) Geotechnical investigation report for the proposed KACST and KSU project, 60 p.

Susilo A, Wiyono S (2012) Frequency analysis and seismic vulnerability index by using Nakamura methods at a new artery way in Porong, Sidoarjo, Indonesia. Int J Appl Phys Math 2(4):227–230

Vaslet D, Al-Musllem M, Maddah S, Brosse JM, Foumiguet J, Breton JP, Le Nindre YM (1991) Geologic map of the Ar Riyad quadrangle, sheet 24 I, Kingdom of Saudi Arabia (without Landsat base): Saudi Arabian Deputy Ministry for Mineral Resources. Jeddah, Geoscience Map GM-121 C.

Ventura CE, Onur T, Hao Ken X.-S (2004) Site period estimations in the fraser river delta using microtremor measurements - experimental and analytical studies. 13th World Conference on Earthquake Engineering, Vancouver, Canada, August 1–6, 2004, Paper No. 1075

Vincent (2008) Saudi Arabia: an environmental overview. Taylor & Francis